# Kinetic description of non-Boltzmann OH rotational distribution in nonequilibrium stationary plasmas

Marco Antonio Ridenti,* Jayr de Amorim,† and Arnaldo Dal Pino
*Department of Physics, ITA - Technological Institute of Aeronautics, São José dos Campos 12228-900, Brazil*

(Received 5 October 2018; published 7 March 2019)

We present a model that describes the departure from equilibrium of the OH(A) rotational level distribution in collisional plasmas. In this model, the OH(A) rotational state densities are governed by a rate equation including: (i) a balanced rotational energy transfer process with the buffer gas species; (ii) unbalanced exothermic reactions, which pump rotationally excited states into the system. Based on the prior assumptions, we formally derive a model function describing the non-Boltzmann distribution. This function depends on five parameters, each of which has a physical meaning. The temperature is given as one of the model function parameters, which can be readily identified with the translational temperature of the buffer gas. The validity of the model was tested by means of the least-squares fitting of data found in literature. Based on this analysis we propose the formation processes of rotationally excited OH(A) in several discharge conditions.

DOI: 10.1103/PhysRevE.99.033202

## I. INTRODUCTION

Measurement of OH (A, $X$) emission spectra from plasmas and hot gases has been used for decades as a technique to estimate the gas temperature [1]. When a rotational distribution is governed by a Boltzmann distribution, its temperature can be determined from the slope of the log plot of the spectrum intensities divided by some other parameters, which may be calculated from first principles, such as transition probabilities, statistical weight factors, and wavelength [1]. However, laboratory plasmas often operate in the nonthermal regime, where rotational distributions have a non-Boltzmann behavior [2,3]. Fundamental assumptions about equilibrium do not hold in these cases, and temperature inference using the conventional approach, i.e., Boltzmann plot, is invalid.

The departure from equilibrium in these systems is believed to be an image of the formation processes of OH($A\,^2\Sigma^+$) or at least to be influenced by it [2,3]. This effect is more pronounced in low-pressure systems, where rotational energy transfer (RET) rates are lower than RET rates in atmospheric pressure plasmas (APPs) [2,3]. Still, molecular spectra from APPs may also exhibit non-Boltzmann behavior [3,4].

This non-Boltzmann distribution has been frequently interpreted as a superposition of distributions with different temperatures [5]. However, this physical interpretation is inconsistent with the foundations of equilibrium thermodynamics and statistical physics. Indeed, if distinct macroscopic systems with different temperatures are put into contact and form an isolated system, the equilibrium condition imposes an equal final temperature [6]. The condition of maximum entropy applied to discretized systems of noninteracting identical particles necessarily leads to a Boltzmann distribution with only one temperature [7]. One could possibly argue that different sets of states couple with distinct thermal baths, but still the maximum entropy principle would require only one mean temperature. Even in the grand canonical ensemble, which better describes a system of a variable number of particles, the resulting distribution is characterized by only one temperature. However, equilibrium thermodynamics cannot be used to predict relaxation times, which could be arbitrarily large in metastable systems. Undoubtedly, the multitemperature picture cannot be explained by the well-established equilibrium statistical physics, but it could eventually be explained by other theories. Multitemperature methods may be useful to indicate nonequilibrium behavior; but apparently it still lacks a universally accepted explanatory theory.

In a previous work, Tsallis nonextensive statistics was used to circumvent this problem [8]. The authors showed that non-Boltzmann behavior observed in $N_2^+$ first negative system spectra can be fitted using a single Tsallis distribution with errors as small as the ones obtained when the fit was carried out using a two-temperature Boltzmann distribution [8]. However, the adoption of this procedure may find some resistance in the plasma community as the foundations of Tsallis nonextensive statistics is still controversial [9–11], even though the balance seems to be pending in favor of the new theory [12]. Another issue contributing to the reluctance of many applied scientists is the large number of unconventional statistical mechanics in vogue [13]. Moreover, there seems to be no clear physical interpretation connecting the $q$ parameter and the associated $q$ entropy to microscopic phenomena in collisional plasmas.

We would like to highlight a method proposed recently by Voráč *et al.* [14]. In order to deal with non-Boltzmann behavior in large spectroscopic data sets with molecular spectra superposition from different molecular bands the authors proposed a state-to-state fitting procedure. The relative population of each excited state is treated as a parameter to be determined in the fitting procedure. The Boltzmann plot is then computed using the calculated populations. The resulting fitting parameters are taken as the starting point for the study

*marcoridenti@gmail.com
†jayr.de.amorim@gmail.com

 

of the non-Boltzmann behavior of rotational distributions. However, this procedure does not solve the problem of the non-Boltzmann distribution; it is just an improved method to compute the Boltzmann plot, since it can deconvolve all the superposed lines that otherwise would have to be discarded.

Fortunately, we can always analyze a system starting from its microscopic dynamics. If a microscopic model gives a good description of the system, we may eventually derive its macroscopic properties, which should be universally valid even when the conditions of thermodynamic equilibrium are not fulfilled. The kinetic theory of gases, for instance, is a good example of this approach. In this paper, we show how the rotational non-Boltzmann distribution of OH(A $^2\Sigma^+$) may be derived assuming an unbalanced effective exothermic reaction and a balanced RET process with background gas. This non-Boltzmann distribution is specified by five parameters, to be fitted to data, all having a physical meaning. We show it is still possible to identify one of the parameters with temperature, since RET processes are usually dominant for low rotational energy levels.

The present problem is somewhat related, though not identical, to the effect observed when superrotors ($J > 50$) are produced using optical centrifuges [15,16]. Experimental observation showed that dephased time decay of coherent states increases with rotational number [16,17]. In plasma applications such superrotors and/or coherent states have never been reported. In these cases, observable upper-lying rotational states are below the limit $J = 50$. Besides, exothermic reactions in plasmas are expected to produce only incoherent states. Nonetheless, the analogy is valuable as we may get some physical insight from the comparison of both systems.

In Sec. II the derivation of the non-Boltzmann distribution is fully developed. In Sec. III we show how data can be fitted using this distribution. Finally, in Sec. IV we apply this model to fit some data extracted from recent literature and interpret the physics of the observed distributions.

## II. THEORY

The process of RET in a OH(A, $v = 0$)[1] containing plasma or gas whose dominant species is an arbitrary atom or molecule M may be represented by the equations

$$\mathrm{M}_j + \mathrm{OH(A)}_{i+1} \underset{k'^{\,i,(+)}_{j+1}}{\overset{k^{i+1,(+)}_{j}}{\rightleftharpoons}} \mathrm{M}_{j+1,(+)} + \mathrm{OH(A)}_i \tag{1}$$

$$\mathrm{M}_j + \mathrm{OH(A)}_i \underset{k'^{\,i-1,(-)}_{j+1}}{\overset{k^{i,(-)}_{j}}{\rightleftharpoons}} \mathrm{M}_{j+1,(-)} + \mathrm{OH(A)}_{i-1}, \tag{2}$$

where the subscript $j$ (or $j+1$) means that species M has a kinetic energy $E_j$ (or $E_j + \Delta E^{(+,-)}$) and the subscript $i$ represents the rotational level OH(A, $J = i$). The $(+)$ superscript refers to a transitions of the kind $i+1 \rightleftharpoons i$ and the $(-)$ superscript refers to a transitions of the kind $i \rightleftharpoons i-1$. This exhausts all the possibilities of population and depopulation of a given rotational state $i$ by a RET process. We may define $\Delta E_i^{(+)} = E_{i+1} - E_i = E_{j+1}^{(+)} - E_j$ as the energy exchanged in the collision process 1 and $\Delta E_i^{(-)} = E_i - E_{i-1} = E_{j+1}^{(-)} - E_j$ as the energy exchanged in the collision process 2. The species M may have internal degrees of freedom, but since we are describing a RET process we shall assume that they do not play any role here. However, such internal degrees of freedom may transfer energy in a resonant process such as

$$\begin{aligned}\mathrm{M}^* + \mathrm{H_2O} &\xrightarrow{\Delta\kappa_i} \mathrm{M} + \mathrm{H_2O}^* \\ &\longrightarrow \mathrm{M} + \mathrm{H}^* + \mathrm{OH(A)}_i\end{aligned} \tag{3}$$

The excited species M* could be an electronically excited atom, such as a metastable excited state from a noble gas [18–21], an energetic electron [22], or a photon [23]. In the above equation we considered water molecules to be one of the precursors of the excitation process of OH, but it could also be another molecule such as the OH($X$) or $H_2O_2$. The requirement is that $\mathrm{OH(A)}_i$ must be a product of the reaction, but not a reagent. Reaction (3) must also be exothermic. In this way, reaction (3) may be seen as a process that continuously pumps rotationally excited OH(A) into the plasma, preventing the thermalization of the system through the totally balanced RET process [Eqs. (1) and (2)].

Another important process, which has exactly the same effect as (3), i.e., producing rotationally excited OH(A) states, is the dissociative recombination of water ions, e.g., [24]

$$\begin{aligned} e + \mathrm{H_2O^+} &\longrightarrow \mathrm{OH} + \mathrm{H} \quad \text{or} \\ e + \mathrm{H_3O^+} &\longrightarrow \mathrm{OH} + \mathrm{H}. \end{aligned}$$

These reactions are exothermic and the excess of energy could be shared among rotationally excited OH(A) states, so we may write

$$e + \mathrm{H_2O^+} \xrightarrow{\Delta\kappa_i} \mathrm{OH(A)}_i + \mathrm{H}^* \quad \text{or} \tag{4}$$

$$e + \mathrm{H_3O^+} \xrightarrow{\Delta\kappa_i} \mathrm{OH(A)}_i + \mathrm{H}^*. \tag{5}$$

Evidently, the reactions above may be included within the class of reactions represented by (3), since all of them obey the criterion that $\mathrm{OH(A)}_i$ be a product but not a reagent of the reaction.

There is another assumption implicit in our formulation: the energy distribution of M* has little or no influence in the branching ratio of the rotationally excited OH(A) states. The M* species surely must have enough energy to create an intermediary excited state $H_2O^*$. After it is created, it eventually dissociates, but this process is uncorrelated to the initial energy of M*. Indeed, the M* energy distribution could affect the total rate coefficient of the reaction, but, as we will see, this will be expressed as a fitting parameter of our model. The shape of the formation energy distribution, however, remains unaffected.

In order to understand how reactions of type (3) cause the departure from equilibrium, let us first analyze the dynamics of a system where $\mathrm{OH(A)}_i$ population is totally controlled by the RET process and then introduce the effect of exothermic reactions. If $N_i$ is the density of OH(A) molecules in state $i$,

[1]We will only consider OH(A) molecules in the vibrational ground state, so from now on we will drop ($v = 0$) from the notation.

its time rate of change may be written as

$$\frac{dN_i}{dt} = N_{i+1}\sum_j k_j^{i+1,(+)}[\mathrm{M}_j] - N_i\sum_j k_{j+1}^{'i,(+)}[\mathrm{M}_{j+1}^{(+)}] + N_{i-1}\sum_j k_{j+1}^{'i-1,(-)}[\mathrm{M}_{j+1}^{(-)}] - N_i\sum_j k_j^{i,(-)}[\mathrm{M}_j], \quad (6)$$

where the $[\mathrm{M}_j]$ is the density of species M with kinetic energy $E_j$, and the summation is taken over the kinetic energy for an arbitrary small $\Delta E_i^{(+,-)}$[2]. Now we introduce the notation

$$k_{i+1}^{(+)} = \sum_j k_j^{i+1,(+)}[\mathrm{M}_j];\ \frac{d}{dE}k_i^{(+)} = \sum_j \frac{d}{dE}k_j^{i,(+)}[\mathrm{M}_j]$$

$$\frac{d}{dE}k_{i-1}^{(-)} = \sum_j \frac{d}{dE}k_j^{i-1,(-)}[\mathrm{M}_j];\ k_i^{(-)} = \sum_j k_j^{i,(-)}[\mathrm{M}_j]$$

and the approximation

$$k_{j+1}^{i\pm1,(\pm)} = k_{j+1}^{i(\pm)} \pm \Delta E_i^{(\pm)}\frac{d}{dE}k_{j+1}^{i,(\pm)}.$$

The $N_i$ time rate of change may be written now as

$$\frac{dN_i}{dt} = (N_{i+1}k_{i+1}^{(+)} - N_i k_i^{'(+)}) - (N_i k_i^{(-)} - N_{i-1}k_{i-1}^{'(-)}) = \left(\frac{dN_i}{dt}\right)^{(+)} + \left(\frac{dN_i}{dt}\right)^{(-)}. \quad (7)$$

We can safely assume microscopic reversibility and a Maxwellian distribution for species M, so we may write [25]

$$\frac{k_i^{'(\pm)}}{k_{i+1}^{(\pm)}} \approx e^{-\frac{\Delta E_i^{(\pm)}}{k_B T}}, \quad (8)$$

where the approximation symbol was used because we consider $g_{i+1}/g_i \approx 1$. The balance equation can be written now as

$$\left(\frac{dN_i}{dt}\right)^{(+)} = N_{i+1}k_{i+1}^{(+)} - N_i k_i^{(+)} + \Delta E_i^{(+)}N_i\left(\frac{k_i^{(+)}}{k_B T} - \dot{k}_i^{(+)}\right) + O((\Delta E)^2) \quad (9)$$

$$\left(\frac{dN_i}{dt}\right)^{(-)} = -\left[N_i k_i^{(-)} - N_{i-1}k_{i-1}^{(-)} + \Delta E_i^{(-)}N_i\left(\frac{k_i^{(-)}}{k_B T} - \dot{k}_i^{(-)}\right) + O((\Delta E)^2)\right]. \quad (10)$$

We look for a solution in the stationary regime, so we may take $dN_i/dt = 0$. If we now divide Eqs. (9) and (10) by $\Delta E_i$ and take the limit $\Delta E_i \to 0$, we obtain

$$\frac{dN}{dE}(k^{(+)} - k^{(-)}) + \frac{N}{k_B T}(k^{(+)} - k^{(-)}) = 0 \Rightarrow \frac{dN}{dE} + \frac{N}{k_B T} = 0, \quad (11)$$

which gives the Boltzmann distribution as the solution, i.e., $N = N_0 \exp(-E/k_B T)$. Note that $N(E)$ is the continuous equivalent to $N_i$, i.e., $N(E_i) = N_i$, where $N(E)$ is now defined for all real values of $E$ between 0 and $\infty$. Although physical values of $E$ are always discrete ($E_i$)—except in the continuum limit—we may always define a continuous $N(E)$ function which best fits experimental points ($E_i$, $N_i$), as long as $N(E_i) = N_i$ is satisfied for every energy level.

Until now we neglected quenching processes, in which a molecule M collides with $\mathrm{OH(A)}_i$ and quenches it. One possible way to account for this effect is to add the term $-\Delta q_i N_i$ in the balance equation, where $\Delta q_i$ is the quenching rate ($\Delta q_i \geqslant 0$). In this case, an analogous procedure would lead us to

$$\frac{dN}{dE} + N\left(\frac{1}{k_B T} - \frac{1}{k}\frac{dq}{dE}\right) = 0, \quad (12)$$

where $k = k^{(+)} - k^{(-)}$. If $Q/k \ll 0$, where $Q = \int_0^\infty (dq/dE)\,dE$, we may neglect the effect of quenching. This approximation is valid for most gases of interest at atmospheric pressure, so we will neglect quenching in this paper and leave it to future works.

We will consider now the effect of the exothermic reactions represented by Eq. (3). First, let us note that the constant $\Delta\kappa_i$ in Eq. (3) should be read as a reaction rate. We represented it using the symbol $\Delta\kappa_i$ for convenience, as we define now the total reaction rate $\kappa_0$ of OH(A) formation at all possible rotational energy levels, i.e.,

$$\mathrm{M}^* + \mathrm{H_2O} \xrightarrow{\kappa_0} \mathrm{M} + \mathrm{H}^* + \mathrm{OH(A)}, \quad (13)$$

where

$$\kappa_0 = \sum_i \frac{\Delta\kappa_i}{\Delta E_i}\Delta E_i \xrightarrow{\Delta E_i \to 0} \kappa_0 = \int_0^\infty \frac{d\kappa}{dE}dE. \quad (14)$$

We will also define $\kappa(E)$ as

$$\kappa(E) = \int_0^E \frac{d\kappa}{dE'}dE',\ \kappa(0) = 0. \quad (15)$$

Let us now introduce the term due to reaction (3) in the balance equation, so that we may write

$$\frac{dN_i}{dt} = \left(\frac{dN_i}{dt}\right)^{(+)} + \left(\frac{dN_i}{dt}\right)^{(-)} + \Delta\kappa_i. \quad (16)$$

Using the same procedure described in the previous case, we now arrive to the following differential equation:

$$\frac{dN}{dE} + \frac{1}{k_B T}N + \frac{1}{k}\frac{d\kappa}{dE} = 0, \quad (17)$$

where $k = k^+ - k^-$. Fortunately, this differential equation has a closed solution, which is

$$N(E) = \left(N_0 + \int_0^E \frac{1}{k}\frac{d\kappa}{dE'}e^{E'/k_B T}dE'\right)e^{-E/k_B T}. \quad (18)$$

[2]Physically, $\Delta E$ cannot be made arbitrarily small, because the OH rotational levels are discretized. Nonetheless, we shall assume that $\Delta E$ can be made arbitrarily small, because we are searching for a continuous function of energy that behaves as the rotational distribution function.

TABLE I. Formulas for the density distribution $N(E)$ for different distributions among exothermic states. The energies $E$ and temperature $T$ are given in eV. The parameter $N_0$ is given in arbitrary units and $\kappa_0/k_0$ must have the same unit as $N_0$.

| Case | $\kappa(E)$ | $N(E)$ |
|---|---|---|
| (i) Heaviside | $\kappa_0 H(E-E_0)$ | $[N_0+(\kappa_0/k_0)e^{E_0/T}]e^{-E/T}$, for $E>E_0$, Boltz. otherwise |
| (ii) Gauss cum. error | $\kappa_0\mathrm{erfc}[-(E-E_0)^2/2\sigma^2]$ | Eq. (21) |
| (iii) Linear | $\kappa_0(E/E_0)$ | $[N_0-(\kappa_0 T/k_0E_0)]e^{-E/T}+(\kappa_0 T/k_0E_0)$ |
| (iv) Quadratic | $\kappa_0(E^2/E_0^2)$ | $[N_0-(\kappa_0 T^2/k_0E_0^2)]e^{-E/T}+(\kappa_0 T/k_0E_0^2)(E-T)$ |

The deviation from equilibrium is governed by the ratio $(1/k)(d\kappa/dE)$. We do not know *a priori* the best function of energy representing this ratio; nonetheless, we may establish an educated guess or *ansatz*.

The rate constant of RET is usually given by an expression, which only depends on $\Delta E$, such as $k = k_0\exp[-(\Delta E)/(k_BT)]$ [26,27]. We immediately verify that this expression converges to a constant value when $\Delta E \to 0$. Our problem now reduces to finding $d\kappa/dE$.

We know that any function of energy, which might represent $\kappa$, i.e., $\kappa=\kappa(E)$, must satisfy the conditions $\kappa(E=0)=0$ and $\lim_{E\to\infty}\kappa(E)=\kappa_0$. In exothermic reactions, in general, the final rotational states are not expected to be equally distributed; on the contrary, there should be a more probable final set of rotational states.[3] Considering these requirements, we may conveniently parametrize $\kappa(E)$ as

$$\kappa(E)=\kappa_0\mathrm{erfc}\left(\frac{E-E_0}{\sqrt{2}\sigma}\right), \tag{19}$$

whose derivative is

$$\frac{d\kappa}{dE}=\frac{\kappa_0}{\sqrt{2\pi\sigma^2}}e^{-\frac{(E-E_0)^2}{2\sigma^2}}. \tag{20}$$

This expression can be interpreted as the energy probability function of the final rotational states, which is given by a Gaussian distribution. If nothing is known *a priori* about the distribution, the central limit theorem guarantees that this should be the best choice.[4] The Eq. (18) can be written now as

$$N(E)=\left\{N_0+\frac{\kappa_0}{k_0\sqrt{2\pi\sigma^2}}\int_0^E\exp\left[-\frac{(E'-E_0)^2}{2\sigma^2}\right]\exp\left(\frac{E'}{k_BT}\right)dE'\right\}e^{-\frac{E}{k_BT}}. \tag{21}$$

This is our key result, which will be used as the model function in the fitting procedure of spectroscopic data described in the next section.

We could generalize Eq. (21) to account for distinct exothermic processes. As a matter of fact, if more than one exothermic process occurs in a given circumstance, Eq. (21) may be insufficient. In some cases, the different exothermic processes may be superposed, if all have similar $E_0$ values. In this case, we may use Eq. (21) to fit a nonequilibrium distribution. However, if $E_0$ values are distinguishable, then Eq. (21) could be generalized and written as

$$N(E)=\left\{N_0+\frac{\kappa_{01}}{k_{01}\sqrt{2\pi\sigma_1^2}}\int_0^E\exp\left[-\frac{(E'-E_{01})^2}{2\sigma_1^2}\right]\exp\left(\frac{E'}{k_BT}\right)dE' + \frac{\kappa_{02}}{k_{02}\sqrt{2\pi\sigma_2^2}}\int_0^E\exp\left[-\frac{(E'-E_{02})^2}{2\sigma_2^2}\right]\exp\left(\frac{E'}{k_BT}\right)dE'\right\}e^{-\frac{E}{k_BT}} \tag{22}$$

in the case of two exothermic processes. The above equations can be readily generalized for any number of exothermic (or formation) processes.

Before proceeding with the application of this formalism to experimental data, let us study some particular solutions of Eq. (18) given a well-defined distribution of energy among the final states, $d\kappa/dE$. We have already done this for the case where $d\kappa/dE$ is proportional to a Gaussian. Let us now plot the solution for this and other cases given a reasonable set of prescribed parameters. This should give us an insight of the dependence of the density distribution on $\kappa(E)$.

Table I shows the four different functions representing $\kappa(E)$. The first case (i) describes the limit in which only one energy state is pumped by exothermic processes. It is equivalent to the Gaussian case in the limit of $\sigma\to 0$. The second case (ii) is the Gaussian distribution of final states, which is considered in this work as the most realistic model. Cases (iii) and (iv) correspond to a linear and quadratic dependence of $\kappa(E)$ on energy or, equivalently, a constant (iii) or linear (iv) distribution of energy among final states.

[3]The average energy of the more probable rotational states, which we may call $E_0$, should scale with the total energy provided by the reaction.

[4]If only one rotational state was excited after the reaction, then we could write $\kappa=\kappa_0 H(E-E_0)$, where $H(E-E_0)$ is the Heaviside function. This is a very particular case, which does not describe correctly our problem in general. Indeed, the expression we propose here reduces to this particular case if $\sigma\to 0$.

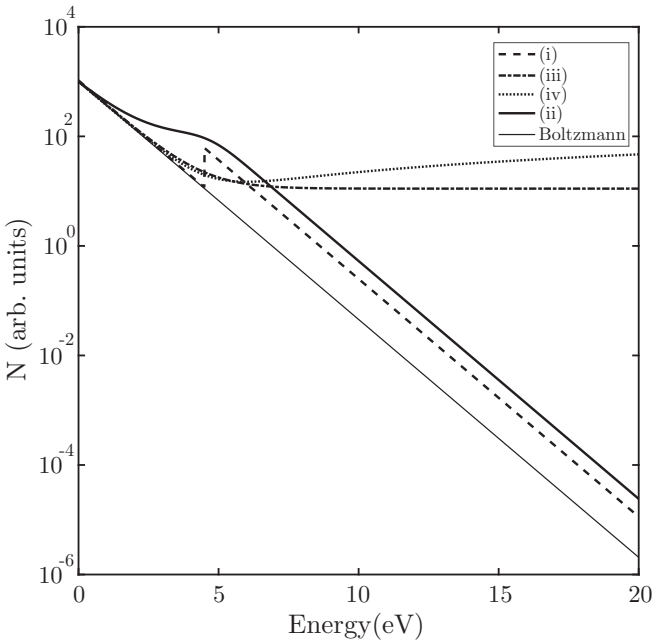


FIG. 1. Density distribution function $N(E)$ for each of the four cases listed in Table I. The prescribed parameters are $E_0 = 4.5$ eV, $T = 1.0$ eV, $\sigma = 0.6$, $N_0 = 1000.0$, and $\kappa_0/k_0 = 50$. The equivalent Boltzmann distribution is also shown.

In Fig. 1 we plot the density distribution for each of the four cases mentioned above (see Table I). In this plot, the prescribed parameters are $E_0 = 4.5$ eV, $T = 1.0$ eV, $\sigma = 0.6$, $N_0 = 1000.0$, and $\kappa_0/k_0 = 50$. We readily verify that all distributions converge to the equilibrium one at low energies, as expected. The idealized limit, in which only one state is populated after the exothermic process, gives rise to a distribution with a positive discontinuity. The derivative of $N(E)$ for $E > E_0$ remains the same, so the effective temperature is always $T$. If the distribution among final states is Gaussian, then a similar deviation from equilibrium is observed, though it deviates continuously. The apparent temperature near $E_0$ increases [the derivative of $N(E)$ decreases for $E < E_0$], and then decreases again until recovering the value $T$ when $E \gtrsim E_0 + \sigma$. This local decrease in the distribution derivative may give rise to an apparent second temperature $T_2$, with no physical meaning, always higher than the real one (the temperature of the dominant gas in equilibrium). The density distribution in the linear case (iii) converges to a constant value $(\kappa_0 T/k_0 E_0)$ for large energies $(E > E_0)$, while in the quadratic case (iv) it diverges linearly.

## III. FITTING PROCEDURE

The fitting procedure was based on the least-squares method, which consists of minimizing the function $\chi^2$ with respect to some set of parameters $\{\beta_i\}$. The $\chi^2$ function is defined as

$$\chi^2 = \sum_i \left( \frac{y_i - f(E_i, \boldsymbol{\beta})}{\sigma(y_i)} \right)^2, \tag{23}$$

where $\{E_i, y_i\}$ is a Boltzmann plot data set, $\sigma(y_i)$ is the data uncertainty and $f(E_i, \boldsymbol{\beta})$ is the model function. From (21) we

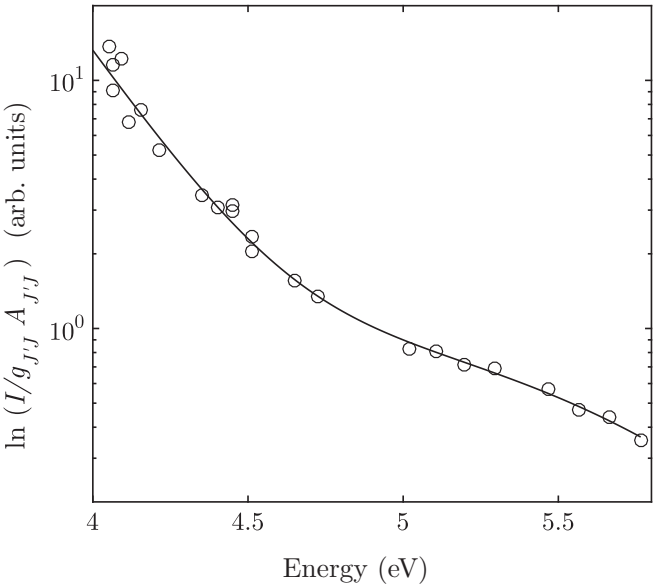


FIG. 2. Fitting curve of the OH(A) Boltzmann plot obtained from the optical emission spectroscopy of a discharge in water vapor bubble with air present as an impurity [30]. The data was extracted from the work of Bruggeman *et al.* [30].

may write the model function explicitly as

$$N(E) = \left\{ \beta_1 + \int_0^E \beta_2 \exp\left[ -\frac{(E' - \beta_3)^2}{2\beta_4^2} \right] \exp\left( \frac{E'}{\beta_5} \right) dE' \right\} e^{-\frac{E}{\beta_5}}. \tag{24}$$

Each parameter of this equation should be related to some of the physical parameters in Eq. (21); the parameter $\beta_1$ is proportional to $N_0$, the parameter $\beta_2$ is proportional to $\kappa_0/(k_0\sigma)$, $\beta_3$ is equal to $E_0$, $\beta_4$ is equal to $\sigma$ and $\beta_5$ is equal to $k_B T$. The function (24) is not linear in the parameters $\{\beta_i\}$ and it must be solved numerically. We used the Gauss-Marquardt-Levenberg algorithm [28] to solve the nonlinear problem of minimizing the $\chi^2$ function. The evaluation of the integral in expression (24) was carried out using the MATLAB® built-in routine of adaptive quadrature [29]. The Gauss-Marquardt-Levenberg algorithm was implemented in MATLAB®.

## IV. RESULTS

In order to verify the consistency of the model function, we fitted some sets of data from a review by Bruggeman *et al.* [3] on that topic. In these figures, we plot the logarithm of the experimental optical emission intensity of the rovibrational transition, $I$, divided by the statistical weight, $g_{J'J}$, and the Einstein coefficient $A_{J'J}$ of the transition. This quantity is proportional to the density of OH(A) rotationally excited states $N_{J'}$ (or $N_i$, in our notation). We simply extracted the data from the paper, without any further data processing. The fitted curves are shown in Figs. 2–5 and the resulting parameters are shown in Table II. The curves fit the concavities of the data, such as in the Boltzmann plot of Fig. 4 and Fig. 5. These concavities can be interpreted as a direct effect of newborn energetic rotational states governed by Gaussian distributions, which originates from exothermic processes creating rotationally excited OH(A).

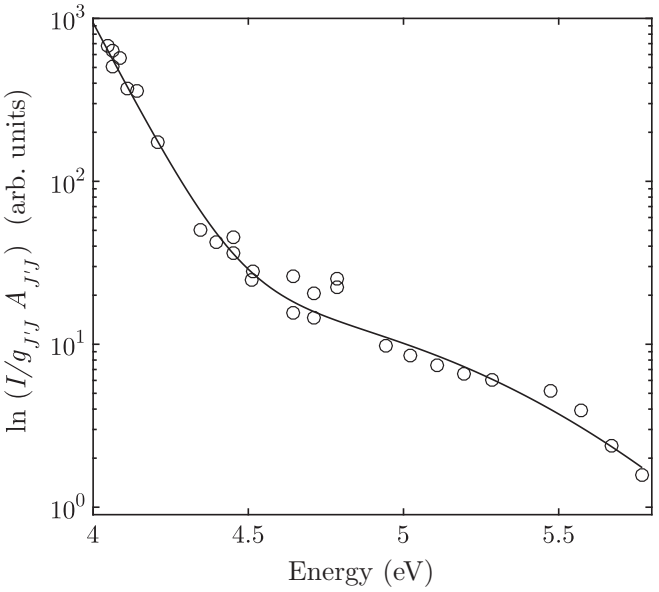


FIG. 3. Fitting curve of the OH(A) Boltzmann plot obtained from the optical emission spectroscopy of a He + 0.1%$N_2$ discharge produced at a current of 25 mA and voltage of 0.9 kV [31]. The data was extracted from the work of Bruggeman *et al.* [31].

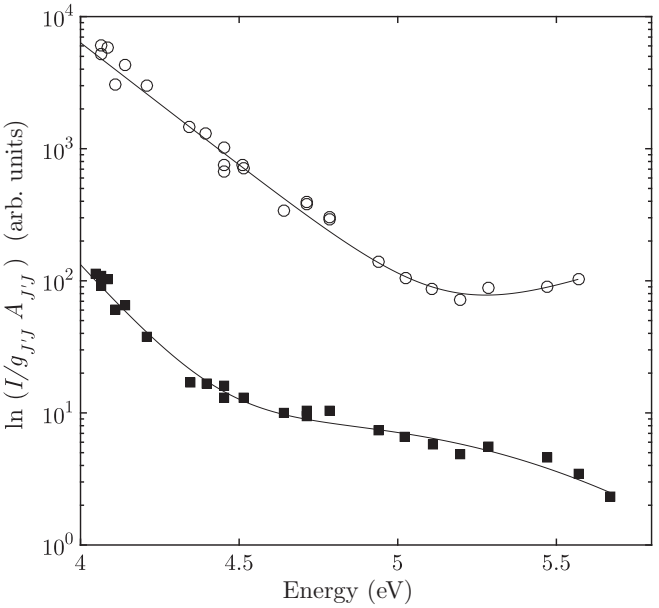


FIG. 5. Fitting curve of the OH(A) Boltzmann plot obtained from the optical emission spectroscopy of a $O_2$ discharge at 760 torr (○) and 25 torr (■) [3]. The data was extracted from the work of Bruggeman *et al.* [3].

The discussion about the physics of these discharges is done in detail by Bruggeman *et al.* [3], so we do not have much more to add than some few words. First, the present treatment gives a precise meaning to the claim that says the departure from equilibrium is an image of the formation processes of OH(A $^2\Sigma^+$). In fact, the model includes the effect of the rotationally excited levels of OH(A) formed just after a chemical or photochemical process. It explains the observed overpopulated rotational states. Besides, the model function contains the term and parameters, which accounts for this effect.

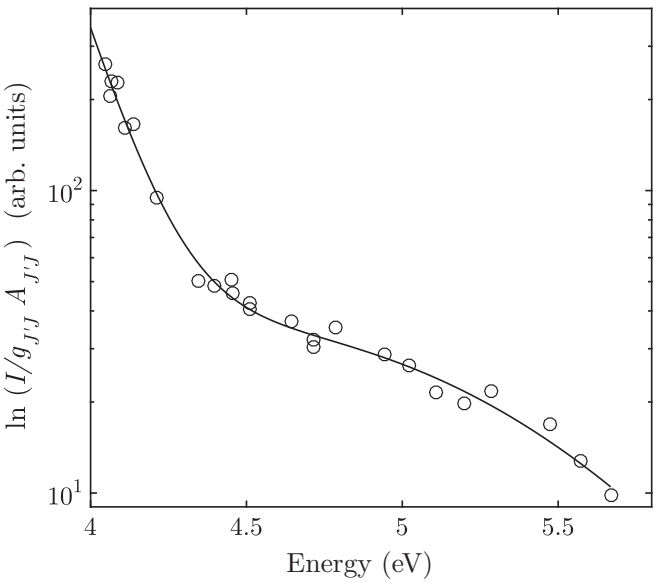


FIG. 4. Fitting curve of the OH(A) Boltzmann plot obtained from the optical emission spectroscopy of a He discharge at 25 torr [3]. The data was extracted from the work of Bruggeman *et al.* [3].

In the present form, the model does not prescribe any temperatures other than the assumed gas temperature $T$. Therefore, we may readily identify the temperature in the model function with the translational temperature of the buffer gas. Some uncertainties may arise if the RET rate is not large enough to overcome the newly born rotationally excited states and the distribution becomes highly non-Boltzmann for all states. However, this situation is more an exception than a rule.

Table II shows the parameters from the fittings presented in Figs. 2–5. The temperatures can be determined with good accuracy and the values are consistent with the ones determined by Bruggeman *et al.* [3] from the straight line fitting of a subset of low rotational energy points. Actually, we used the latter as the initial guess of the nonlinear fitting.

We also analyzed the data of Voráč *et al.* [14] and the fitting curve is shown in Fig. 6. The fitting parameters are shown in Table III. Here again, we found good agreement between $T$ and $T_1$ determined by Voráč *et al.* [14]. In this case, the concavity of the overpopulated tail is very clear, but we observe more than one ripple. This behavior is consistent with a description that considers two exothermic processes with very different mean output energies. In this case, the model function may be written as

$$N(E) = \left\{\beta_1 + \int_0^E \beta_2 \exp\left[-\frac{(E'-\beta_3)^2}{2\beta_4^2}\right]\exp\left(\frac{E'}{\beta_8}\right) + \beta_5 \exp\left[-\frac{(E'-\beta_6)^2}{2\beta_7^2}\right]\exp\left(\frac{E'}{\beta_8}\right)dE'\right\}e^{-\frac{E}{\beta_8}}. \tag{25}$$

We truncated the data above 4.8 eV, because the dispersion increases beyond that point. This case is especially interesting,

TABLE II. Parameters obtained from the fitting procedure, for each data set extracted from the review of Bruggeman *et al.* [3]. Estimates of errors are shown using parentheses notation [32]. Results from the two different curves of Fig. 5 are indicated using the shapes of the data points (○ or ■).

| Fig./Ref. | $\beta_2$(1/eV) | $\beta_3$(eV) | $\beta_4$(eV) | $T$($10^3$ K) | $T$($10^3$ K)[a] [3] |
|---|---|---|---|---|---|
| 2/[30] | 2.86(34) | 4.68(15) | 0.71(10) | 2.88(12) | –[b] |
| 3/[31] | 130.0(35) | 4.27(35) | 0.652(14) | 1.380(18) | 1.33(30) |
| 4/[3] | 250.3(35) | 4.333(38) | 0.779(25) | 1.566(59) | 1.94(30) |
| 5(○)/[3][c] | 0.4(14) $\cdot 10^4$ | 7.6(32) | 1.05(70) | 2.715(25) | 2.91(30) |
| 5(■)/[3] | 46.36(53) | 4.617(19) | 0.587(15) | 1.897(49) | 2.00(30) |

[a]The authors of the original work omitted the uncertainties for these values; we chose the highest error values reported in Ref. [3].
[b]In this case Bruggeman *et al.* fits three temperatures, so any comparison is uncertain [3].
[c]This data set is not complete enough for convergence; the parameters $\beta_2$, $\beta_3$, and $\beta_4$ cannot be determined accurately.

because we may use the fitting parameters to infer which exothermic processes are responsible for each ripple, as we will see later.

It is in principle possible to determine $\kappa_0/k_0$ from fitted values and compare it with experimental or theoretical values. This would possibly allow us to determine the most probable formation process in each case. However, as far as we are concerned, there are no theoretical or experimental values of $\kappa_0$. We may find estimates of the total rate coefficient of electron-ion dissociative recombination of water, which accounts for all possible final states of OH [24]. This would be insufficient, however, since we need a reliable estimate of the branching ratio for the formation of OH(A). On the other hand, we may find some rough estimates of $k_0$ for many RET processes in literature, but we would still need $\kappa_0$. Besides, $\beta_3$, $\beta_4$, and $\beta_5$ parameters could be highly correlated so that our estimate of $\kappa_0/k_0$ would be very likely imprecise.

Fortunately, we may use $\beta_3$ (and $\beta_6$, if it is the case) to establish an educated guess about the formation processes leading to overpopulation of excited states. The data of

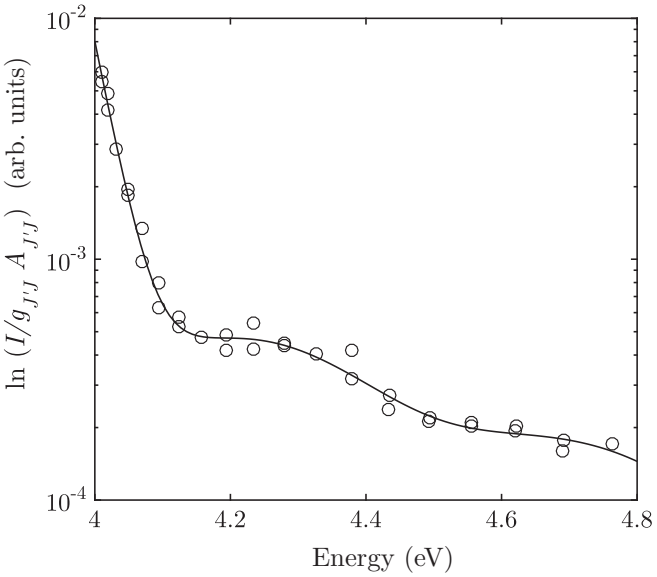


FIG. 6. Fitting curve of the OH(A) Boltzmann plot obtained from the optical emission spectroscopy of a dielectric barrier discharge (DBD) in water-argon interface at atmospheric pressure [14]. The data was extracted from the work of Voráč *et al.* [14].

Voráč *et al.* [14] presented two ripples, as we have just shown (see Fig. 6), each of which is associated with an average energy $\beta_3 = 4.180(6)$ eV and $\beta_6 = 4.644(19)$ eV. This discharge was produced in an environment of argon saturated with water vapor at atmospheric pressure. We may identify two high rate coefficient exothermic reactions under such circumstances: (i) water vapor dissociative recombination [reactions (4) and (5)]; (ii) and dissociation by metastable atoms ($Ar_m$). The estimated reaction energies are $\Delta E \approx 7.5$ eV for (i) and $\Delta E \approx 6.6$ eV for (ii). Both reactions may excite OH(A), whose minimum electronic energy is ∼4.0 eV [1]. Reaction (i) is more energetic, so we may assign the second ripple to water vapour dissociative recombination and the first ripple to process (ii).

The proposed assignment is also consistent with the data of Bruggeman *et al.* [3]. The estimated value of $E_0$ in a water bubble plasma was $\beta_3 = 4.68(25)$ eV (see Table II). This value is compatible with $\beta_6$ (Voráč *et al.* data), as expected, since (i) is the most probable exothermic process in the water bubble case.

We may also explain the formation of OH(A) on helium discharges based on our analysis. The estimated values of $E_0$ are mutually consistent, whether or not a small percentage of $N_2$ is present (see Table II). In this case, a probable mechanism is charge exchange,

$$He_2^+ + H_2O \longrightarrow OH + HeH^+ + He. \qquad (26)$$

The reaction energy is ∼5.6 eV, which is also large enough to excite OH(A). The estimated $E_0$ values are lower than $\beta_6$, so that a mechanism other than water vapor dissociative recom-

TABLE III. Parameters obtained from the fitting procedure for the data extracted from the work of Voráč *et al.* [14]. Estimates of errors are shown using parentheses notation [32].

| Parameter | Value |
|---|---|
| $\beta_2$ | 0.01505(3) $eV^{-1}$ |
| $\beta_3$ | 4.180(6) eV |
| $\beta_4$ | 0.164(8) eV |
| $\beta_5$ | 0.00576(13) $eV^{-1}$ |
| $\beta_6$ | 4.644(19) eV |
| $\beta_7$ | 0.207(22) eV |
| $T$ | 351(7) K |
| $T_1$ [14] | 343(28) K |

bination takes place in this case. Charge exchange seems to be the only one that satisfies all the requisites.

## V. CONCLUSION

In this work we developed a model to describe the departure from equilibrium of the OH(A) rotational level distribution generated in collisional plasmas. It assumes that OH(A) rotational state densities are governed by a rate equation including the balanced RET process with the buffer gas species plus a single unbalanced exothermic reaction, which pumps rotationally excited states into the system. Based on the former, we formally derived a function of energy that describes the non-Boltzmann distribution. This function depends on five parameters, each of which has a physical meaning. The validity of the model was tested by means of the least-squares fitting of data relating to different discharge conditions [3]. All the tested data could be fitted satisfactorily using the present theory.

The present method is based on a theory that takes into account the processes of formation of OH(A) rotationally excited states. It assumes a buffer gas in thermal equilibrium, with a well-defined temperature. In the present formulation, the theory does not prescribe other temperatures.

Using this theory we were able to describe the ripples in experimentally obtained rotational distributions, which we interpreted as the effect of rotationally excited states pumped into the system due to formation processes. In a very interesting case (Voráč *et al.* [14]) two ripples were clearly distinguishable. From our analysis and previous knowledge about buffer gas composition, we assigned a formation process to each ripple. We also proposed the main mechanisms leading to OH(A) formation in discharges at other conditions [3].

The present theory is not complete because it neglects some effects, which may be important depending on the discharge conditions. One of them is the quenching effect, which we briefly mentioned in Sec. II. Another is the electron impact excitation of OH. In this case, the OH(A) rotational distribution may be coupled to the electron energy distribution. A two-temperature distribution is possible in this case. These effects could be included in a more general version of this model. Another possible development is the treatment of the nonstationary case, which may be used to understand subnanosecond resolved spectra. We leave these as suggestions for future investigations.

## ACKNOWLEDGMENTS

M.A.R. would like to thank the Brazilian National Council for the Improvement of Higher Education for the support of a scholarship under Grant No. CAPES/ITA 005/2014, which enabled him to carry out this work.

[1] G. Dieke and H. Crosswhite, J. Quant. Spectrosc. Radiat. Transfer **2**, 97 (1962).
[2] P. Bruggeman, N. Sadeghi, D. Schram, and V. Linss, Plasma Sources Sci. Technol. **23**, 023001 (2014).
[3] P. Bruggeman, D. C. Schram, M. G. Kong, and C. Leys, Plasma Processes Polym. **6**, 751 (2009).
[4] M. A. Ridenti, J. A. Souza-Corrêa, and J. Amorim, J. Phys. D: Appl. Phys. **47**, 045204 (2014).
[5] V. Linss, Spectrochim. Acta, Part B **60**, 253 (2005).
[6] L. Landau and E. Lifchitz, *Physique Statistique* (Éditions Mir., Moscou, 1967).
[7] K. Huang, *Introduction to Statistical Physics* (CRC Press, Boca Raton, 2009).
[8] J. L. Reis, J. Amorim, and A. Dal Pino, Phys. Rev. E **83**, 017401 (2011).
[9] M. Nauenberg, Phys. Rev. E **67**, 036114 (2003).
[10] C. Tsallis, Phys. Rev. E **69**, 038101 (2004).
[11] M. Nauenberg, Phys. Rev. E **69**, 038102 (2004).
[12] J. Cartwright, Physics World **27**, 31 (2014).
[13] R. Luzzi, Á. R. Vasconcellos, and J. G. Ramos, arXiv:cond-mat/0412233.
[14] J. Voráč, P. Synek, V. Procházka, and T. Hoder, J. Phys. D: Appl. Phys. **50**, 294002 (2017).
[15] J. Karczmarek, J. Wright, P. Corkum, and M. Ivanov, Phys. Rev. Lett. **82**, 3420 (1999).
[16] A. Korobenko, A. A. Milner, and V. Milner, Phys. Rev. Lett. **112**, 113004 (2014).
[17] A. A. Milner, A. Korobenko, J. W. Hepburn, and V. Milner, Phys. Rev. Lett. **113**, 043005 (2014).
[18] M. Clyne, J. Coxon, D. Setser, and D. Stedman, Trans. Faraday Soc. **65**, 1177 (1969).
[19] Y. Golubovskii, D. Kalanov, and V. Maiorov, Phys. Rev. E **96**, 023206 (2017).
[20] M. A. Ridenti, J. de Amorim, A. Dal Pino, V. Guerra, and G. Petrov, Phys. Rev. E **97**, 013201 (2018).
[21] Y. Kabouzi, D. B. Graves, E. Castaños-Martínez, and M. Moisan, Phys. Rev. E **75**, 016402 (2007).
[22] C. Beenakker, F. De Heer, H. Krop, and G. Möhlmann, Chem. Phys. **6**, 445 (1974).
[23] T. Carrington, J. Chem. Phys. **41**, 2012 (1964).
[24] P. Bruggeman and D. C. Schram, Plasma Sources Sci. Technol. **19**, 045025 (2010).
[25] M. H. Alexander, Lecture notes and instructional material in theoretical chemistry (2010), http://www2.chem.umd.edu/groups/alexander/teaching/index.html.
[26] M. L. Koszykowski, L. A. Rahn, R. E. Palmer, and M. E. Coltrin, J. Phys. Chem. **91**, 41 (1987).
[27] D. A. Kliner and R. L. Farrow, J. Chem. Phys. **110**, 412 (1999).
[28] O. Helene, *Método dos Mínimos Quadrados com Formalismo Matricial*, 1st ed. (Editora Livraria da Física, Sao Paulo, 2006).
[29] L. F. Shampine, J. Comput. Appl. Math. **211**, 131 (2008).
[30] P. Bruggeman, D. Schram, M. Á. González, R. Rego, M. G. Kong, and C. Leys, Plasma Sources Sci. Technol. **18**, 025017 (2009).
[31] P. Bruggeman, J. Liu, J. Degroote, M. G. Kong, J. Vierendeels, and C. Leys, J. Phys. D: Appl. Phys. **41**, 215201 (2008).
[32] *Guide to the Expression of Uncertainty in Measurement* (International Organization for Standardization, Geneva, 1995), https://www.bipm.org/utils/common/documents/jcgm/JCGM_100_2008_E.pdf.